

# Low-cost Sonar based on the Echolocation

Thiago Moreira<sup>1</sup><sup>a</sup>, José Lima<sup>2,3</sup><sup>b</sup>, Paulo Costa<sup>3</sup><sup>c</sup> and Márcio Cunha<sup>1</sup><sup>d</sup>

<sup>1</sup>Academic Department of Electronic, Federal University of Technology, Paraná, Brazil

<sup>2</sup>CeDRI - Research Centre in Digitalization and Intelligent Robotics, Polytechnic Institute of Bragança, Bragança, Portugal

<sup>3</sup>INESC TEC - INESC Technology and Science and Faculty of Engineering of University of Porto, Porto, Portugal

**Keywords:** Object Detection, Echolocation, Sonar, Mobile Robot Navigation.

**Abstract:** In the world of mobile robot navigation, the ultrasonic sensors stand out for presenting attractive features at an affordable cost. The main problem in the use of these devices lies in the difficulty of correctly interpreting the obtained data, which means that their efficiency is limited. This paper focuses on the improvement and implementation of a low cost location system based on ultrasonic sensors. Through the combination of mathematical techniques and signal processing it is possible to make the system more accurate and reliable. The developed system includes the data acquisition, the signal filtering, and the trigonometric methods to estimate the coordinates of a target and can be assembled in a mobile robot.

## 1 INTRODUCTION

One of the great challenges of mobile robot navigation is the detection of targets and their location. Most systems used to solve this task are vision based and sensor (non-vision) based. In the first one, detection through cameras and image processing are subject to a lack of precision, which can arise as a result of variation in environmental conditions like darkness, foggy or low visibility (Patkar and Tasgaonkar, 2016). Moreover, the computational consumption and the price of these systems are still high (Kreczmer, 2010).

The cost-effective of robots is an important feature to consider before the building process. To keep their cost down, expensive sensors and devices should be evaluated. In this way, ultrasonic sensor seems to be suitable to deal with this problem (Wu and Tsai, 2001; Kim and Choi, 2008). It has proven to be very efficient, economical and accurate (Lim et al., 2014).

Systems based on ultrasonic sensor have many advantages over other methods. For example, in applications that require reduced size the modules can be very small without interfering in their performance. In addition, it is capable of operating in sev-

eral environments in which other devices can not be used (Kim and Choi, 2008).

In robotic applications, ultrasonic sensing is rarely used beyond simple functions such as obstacles avoidance. However, some works show just how useful the sensor can be (Schillebeeckx et al., 2011; Popelka et al., 2016). The best known example that use ultrasonic navigation are the bats. They're able to avoid obstacles even at high speeds when flying in the dark (Cheeke, 2016). The main difference between an ultrasonic range finder and the bat is that it has two ears, which allows them to detect which direction the echo comes from (Kreczmer, 2010).

The major drawback of this technique occurs due to the wide beam of an emitted signal, causing a misinterpretation of the object's real reflection. When irregularities of the object surface are much smaller than the wavelength of the signal, there is also the called multiple reflection effect. The last event can be noticed when successive measurements are performed in a regular short time. In an attempt to avoid this problem, a system containing two receivers and a transmitter is required (Kreczmer, 2010).

Inspired by the echo location of the animals, this paper proposes a low cost ultrasonic binaural system based on accuracy techniques and discusses the difficulties associated with the use of ultrasonic measurements in indoor environments.

In section 2, the main distance estimation methods are briefly described. In section 3, a review is made

<sup>a</sup> <https://orcid.org/0000-0002-6132-2914>

<sup>b</sup> <https://orcid.org/0000-0001-7902-1207>

<sup>c</sup> <https://orcid.org/0000-0002-4846-271X>

<sup>d</sup> <https://orcid.org/0000-0001-7506-4488>

about the conventional ultrasonic range system and the binaural sensor system. In section 4, the architecture of the proposed system is presented. In section 5, the method of triangulation using ultrasonic sensors is introduced. In section 6, the results of the experimental tests are reported. Finally, in section 7 the results are discussed and conclusions drawn.

## 2 DISTANCE ESTIMATION METHODS

The main approaches to determine the distance through ultrasonic waves are given by the phase shift and time-of-flight (TOF). The first strategy comprises the continuous calculation of the phase shift between the transmitted and received signal. However, this strategy has a very narrow measurable range. The second strategy, unlike the first one, allows to measure greater distances and consists in determining the time that a wave takes to reach the receiver. The transmitter sends the sound waves to an object or obstacle and, when it is detected, returns to the receiver (Huang and Huang, 2009; Queirós et al., 2006).

There are several methods for estimating the TOF, in the following subsections the most common techniques are presented.

### 2.1 Threshold Detection

This form is the simplest and fastest way to calculate the TOF. It involves transmitting and detecting the arrival of an ultrasonic wave when the received signal exceeds, for the first time, a predefined threshold level, as seen in Figure 1. There are some benefits to using this method, it requires no complex computation and can be performed with simple circuitry. The main problem of this method is that it typically estimates a higher TOF compared to the actual one. This happens due to the long rise time of the signal, added to other factors, such as low signal-to-noise ratio (SNR) and inherent bias (Jackson et al., 2013; Queirós et al., 2006).

As noise increases the likelihood of incorrect readings also increases, and systems that use threshold as a reference value are vulnerable to this type of error. In low SNR conditions, it is recommended to amplify the signal, or equivalently, adjust the detection threshold in order to reduce the system uncertainty. According to (Jackson et al., 2013), the inherent bias occurs for two reasons: the first is that no matter how good the transducer performance is, there will always be a rise time when a signal is detected;

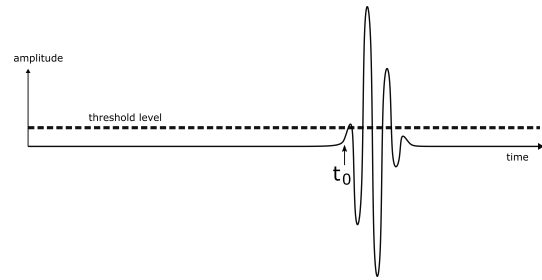


Figure 1: Threshold detection method (Kuc and Siegel, 1987).

the second and most crucial is the threshold level setting, this is a critical factor for the bias, because if a low threshold is set the occurrence of false positives tends to increase.

### 2.2 Cross-correlation

The TOF estimation can be considered as a time delay issue, for instance, suppose an ultrasonic signal  $s_T(t)$  is generated, so when it propagates in the air and is reflected, the time between the transmission and the reception of the signal is given by a delay  $\tau$ . Thus, techniques for calculate the time delay should be used. Among them, cross-correlation has been highlighted (Marioli et al., 1992). Cross-correlation is a quantitative operation in the time domain to relate two signals, when applied between the transmitted and received signal, the result is a peak at the time delay  $t_0$ , as shown in Figure 2. The cross-correlation  $c(t)$  is calculated by:

$$c(t) = \int_{-\infty}^{+\infty} s_T(t)s_R(t+\tau)d(\tau) \quad (1)$$

where  $s_T(t)$  is the transmitted signal,  $s_R(t+\tau)$  is the signal received and shifted in time.

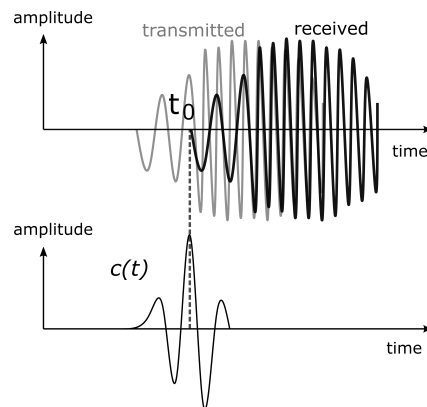


Figure 2: Cross-correlation method. Adapted from (Jackson et al., 2013).

The main disadvantage is that it requires a high computational consumption, and second (Xu et al., 2009) this method is only suitable for slightly dispersive waves, otherwise the method is not so efficient.

### 2.3 Envelope Detection

Envelope detection is an alternative to the other methods mentioned above, which can be assumed as an intermediary version between threshold detection and cross-correlation. In (Xu et al., 2009) a comparison made from the most common procedures of TOF estimation demonstrated that envelope detection obtained satisfactory results, only losing to the cross correlation. However, in terms of computational processing this technique is most convenient.

The envelope detector makes use of the Hilbert Transform to generate an analytical signal, whose absolute value represents the envelope of the measured signal. The analytical signal  $y(t)$  of a real signal  $x(t)$  is defined by:

$$y(t) = x(t) + jh(t) \tag{2}$$

where  $h(t)$  is the Hilbert Transform of  $x(t)$  and  $j = \sqrt{-1}$ . The magnitude of the analytic signal, which is identical to the real signal, is called envelope as seen in Figure 3. Thus, from the envelope extraction it is possible to locate the peaks and determine the time between sending and receiving the echo signal. Hence, the problem of setting the threshold level is eliminated.

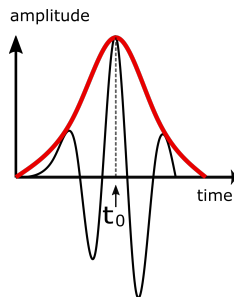


Figure 3: The envelope extraction of the echo signal.

## 3 SENSOR SYSTEM

In the present work the binaural sensor system was adopted to improve the system performance, but before studying how it works in the following subsections a brief analysis of the traditional use of the ultrasonic sensor is presented in order to clarify the difference between these two types.

### 3.1 Conventional Ultrasonic Ranging System

This scheme is basically a conventional TOF system. The standard mode of operation is to transmit an acoustic signal through the air and measure the duration until it is reflected by some object. The distance  $d$  can be obtained from

$$d = \frac{c \cdot T_f}{2} \tag{3}$$

where  $c$  is the sound velocity and  $T_f$  is the TOF (Kuc and Siegel, 1987).

As previously mentioned, the beam width of these sensors is large, which makes it unfeasible to locate the object using just one sensor. Furthermore, only the first reflection is measured in this configuration, making the amount of information obtained extremely limited (Peremans et al., 1993).

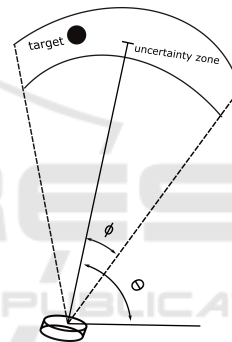


Figure 4: The beam width of a single sensor. Adapted from (Peremans et al., 1993).

### 3.2 The Binaural Sensor System

The binaural sensor arrangement, presented in Figure 5, aims to combine the use of two ultrasonic sensors to provide more detailed spatial information and map the environment. Conforming to (Kreczmer, 2010) the disadvantages of a single sensor are reduced when a multi-sonar system is used. The proposed system consists in three conventional ultrasonic sensors, one of which acts as a transmitter and the other two as a receiver. In this work it is assumed that the propagation of sound waves occurs in a horizontal plane, equivalent to the two-dimensional space. Thus, the location of an object is defined by the region of intersection with the horizontal plane through the sensors A and B, called detection area, as shown in Figure 6.

The receivers, sensors A and B, are separated by a known baseline ( $l$ ) that allows locating the detected objects in a planar environment, estimating the TOF

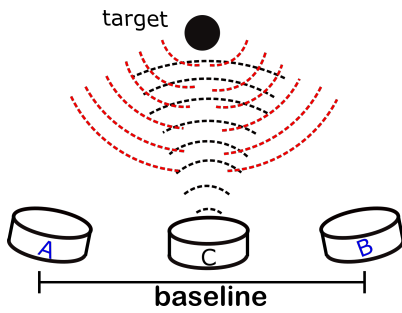


Figure 5: The Binaural sensor arrangement.

between the object and each sensor through the envelope detection. Then, the distance calculation is solved by trigonometric techniques. Fixing the angle and baseline it is also possible to change the detection field when the two ultrasonic beam patterns overlap.

The ideal positioning of the system was defined by the baseline and the  $\alpha$  angle, as can be seen in Figure 6. The maximum width of the detection area occurs when the beam patterns overlap completely, that is, with a close distance and  $\alpha = 90^\circ$ . When the width is small, as in Figure 7b, the behavior is similar to system mentioned in Subsection 3.1. When the width is larger, as shown in Figure 7a, it is possible to expand the coverage area. By adjusting the angle of rotation the points of intersection can increase or decrease, and the mapping of all valid positions for the detection can be made by tracing arcs with fixed distances in the locating cone.

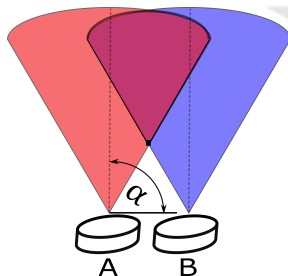


Figure 6: Detection area formed by the beam patterns. Adapted from (Gearhart et al., 2009).

#### 4 SYSTEM ARCHITECTURE

The system is composed by three low-cost ultrasonic sensors HY-SRF05 and a microcontroller STM32F103C8T ARM Cortex-M3 with two built-in analog to digital (A/D) converters. The ultrasonic burst is performed by sensor C and the raw echo signal received by sensors A and B is sent to the 12 bits A/D converters of the microcontroller with a sampling rate of 320 kHz. Assuming the sound velocity

as approximately 340 m/s, it can be stated that the distance is covered 0.034 cm/μs. The reciprocal is equal to 29.412 μs/cm, and considering a round trip corresponds to 58.824 μs/cm. Using this constant it is possible to simplify the determination of the distance and substitute the Equation (3) by the equation below:

$$d = \frac{T_f}{K}, \tag{4}$$

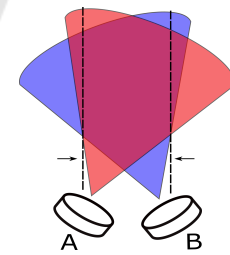
where  $K \approx 59$ .

Four thousand readings are stored from each sensor, which if multiplied by the sampling period,  $T_s = 3.125 \mu s$ , corresponds to a sample space of 12500 μs. Using the Equation (4) we can estimate that the proposed system has a maximum range of about 212 cm depth, that is, along the y-axis. The x-axis is bounded by the established baseline.

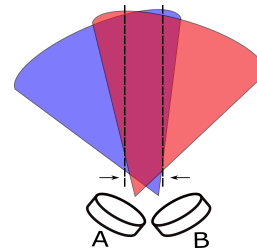
After the data acquisition, the samples are transmitted over RS-232 protocol to the MATLAB, where the envelope extraction and the TOF estimation of sensors A and B are performed. Finally, the calculation of the object coordinates is executed. In order to reduce the noise, a second-order Butterworth band-pass filter was applied in the echo signal. The phase delay produced by the filter was negligible. The system overview is shown in Figure 8.

#### 5 TRIANGULATION

Triangulation is the process of determining the location of a target from known points using trigonometric techniques. Currently, triangulation is applied



(a) Wide overlap region.



(b) Thin overlap region.

Figure 7: Adapted from (Gearhart et al., 2009).

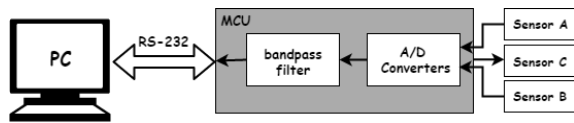


Figure 8: Hardware Implementation.

in several areas, including navigation, metrology and astrometry. Generally, the number of sensors corresponds to the number of dimensions of the estimated position of the object, for example, two sensors can indicate a location in 2D, while three in 3D (Gearhart et al., 2009).

In geometry, there is a formula that allows to calculate the area of any triangle when the lengths of the three sides are known. This approach was discovered by the mathematician Heron of Alexandria (Bényi, 2003). Knowing the distance from the baseline between the sensors and the distance calculated by them, it can be computed the area of the triangle formed using Heron’s formula, as shown in Equation 5:

$$\Delta(abc) = \sqrt{p(p-a)(p-b)(p-c)}, \quad (5)$$

$$p = \frac{a+b+c}{2} \quad (6)$$

whose  $a, b, c$  are the known sides.

Alternatively, the area of a triangle is also given by Equation 7:

$$\Delta(abc) = \frac{b \cdot h}{2} \quad (7)$$

where  $b$  is the base and  $h$  is the height of the triangle.

Rearranging the Equation (7), results in:

$$h = \frac{\Delta(abc) \cdot 2}{b} \quad (8)$$

If the area calculated in Equation 5 is replaced in Equation 8 and the base by the known baseline, it is possible to determine the y-coordinate of the object. Figures 9 and 11 show the nomenclatures adopted for the geometric parameters. The x coordinate can now be calculated if the original triangle is separated into two right triangles and after that the Pythagoras Theorem is applied, according to the Equations 9 and 10:

$$C_1 = \sqrt{d_A^2 - h^2} \quad (9)$$

$$C_2 = \sqrt{d_B^2 - h^2} \quad (10)$$

where  $h, C_1, C_2, d_A$  and  $d_B$  can be seen in Figure 9.

If the Equation (9) is used, the system reference for the coordinates on the x-axis will originate from sensor A otherwise, from sensor B.

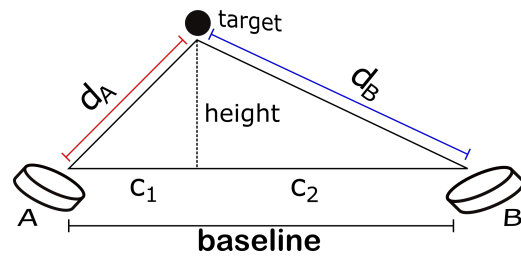


Figure 9: Typical triangulation.

In Figure 4 it is possible to get a perspective of the systems that use a single ultrasonic sensor. Objects can be detected anywhere into uncertainty zone. However, without additional information the system is not able to make a decision to avoid a collision, only that there is an object present in the detection field.

Valid mathematical events but nonsense physical can occur using the equations described previously, such as when two objects are separate but are only detected as one. Therefore, some constraints were defined in order to avoid incoherent data. To prevent the error shown in Figure 10, it was observed that  $\theta_1$  and  $\theta_2$  angles are outside of the detection area.

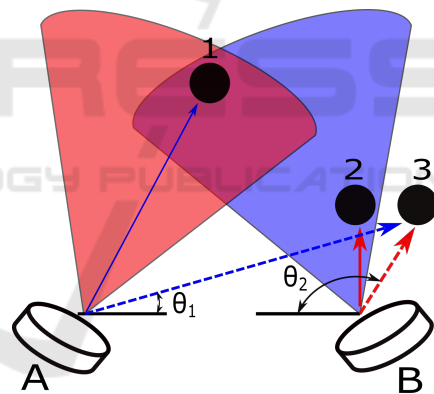


Figure 10: Typical triangulation error. Adapted from (Gearhart et al., 2009).

Figure 10 demonstrates that sensor A detects target 1 and sensor B detects target 2. However,  $\theta_1$  and  $\theta_2$  are outside the triangulation area, which causes a misinterpretation resulting in a wrong coordinate (target 3).

The next equations and the proposed analysis were also established by (Gearhart et al., 2009). Figure 11 demonstrates how  $\theta_1$  and  $\theta_2$  should be for a valid detection region and evidence that  $\theta_1 = \alpha_1 \pm \phi$ . The  $\alpha_n$  is the angular position of the sensor  $n$  relative to the x-axis. The  $\phi$  is half the angle of the detection beam, and is a value specific to each sensor model. The angular limiting interval can be given by:

$\cos(\alpha_1 - \phi) \leq \cos \theta_1 \leq \cos(\alpha_1 + \phi)$ , which

$$\cos \theta_1 = \frac{l^2 + d_A^2 - d_B^2}{2ld_A} \quad (11)$$

Analogously to sensor B, the angular limiting range is given by:  $\cos(\alpha_2 - \phi) \leq \cos \theta_2 \leq \cos(\alpha_2 + \phi)$ , and

$$\cos \theta_2 = \frac{l^2 + d_B^2 - d_A^2}{2ld_B} \quad (12)$$

The  $\alpha_1$ ,  $\alpha_2$  and  $\phi$  are constant, so it is necessary to calculate only  $\cos \theta_1$  and  $\cos \theta_2$ . Readings outside this range are discarded.

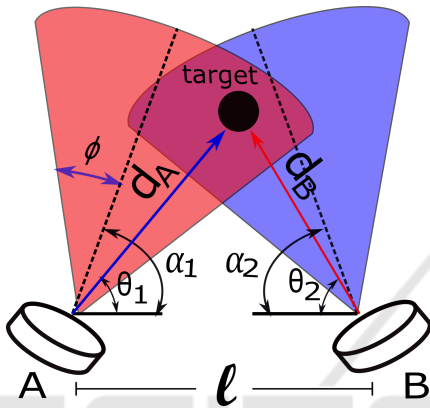


Figure 11: Triangulation created from the sensors. Adapted from (Gearhart et al., 2009).

## 6 RESULTS

The objective of the experimental tests was to analyze the accuracy of the proposed method and the behavior of the developed system. The tests were divided into two situations: the first with only one object and the second with two objects. The following subsections describe the procedures and results obtained.

### 6.1 First Scenario

To perform the tests a small cardboard box was used and the receivers were positioned with  $\theta_{1,2} = 45^\circ$  and  $l = 51 \text{ cm}$ . Measurements were made with the object positioned to the right, left and center of the detection area. Sixty-four samples of each position were collected and the standard deviation ( $\sigma$ ), mean ( $\overline{(x,y)}$ ) and variance ( $\sigma^2$ ) of each were calculated, as can be seen in Table 1. Figures 12, 13 and 14 shows the variation of the samples in relation to the mean of each measurement.

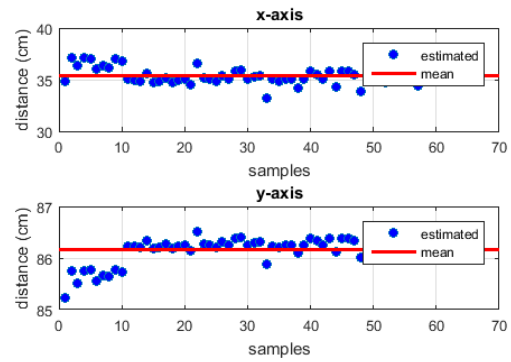


Figure 12: Dispersion of the x-axis and the y-axis samples about the mean value of the box positioned in the right.

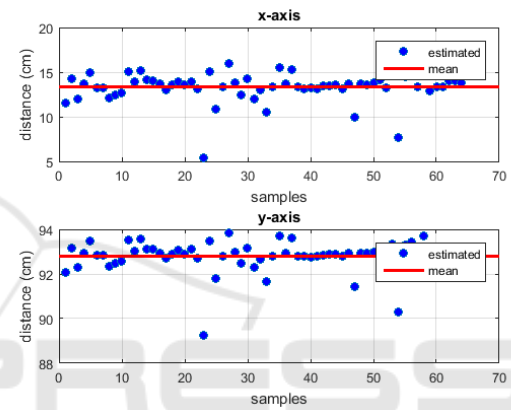


Figure 13: Dispersion of the x-axis and the y-axis samples about the mean value of the box positioned in the left.

### 6.2 Second Scenario

Due to the fact that the raw echo signal is used, a deeper analysis of the environment is possible. When more than one object is present in the scene it is possible to detect it through the peaks of the envelope, as shown in Figure 17. If two objects are very close the

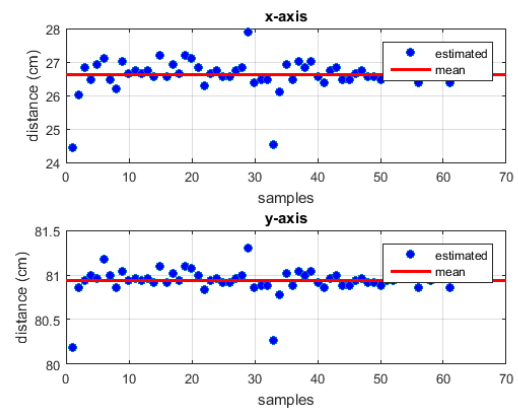


Figure 14: Dispersion of the x-axis and the y-axis samples about the mean value of the box positioned in the center.

Table 1: Mean, standard deviation and variance of the first tests.

Positioning	$(x,y)_{real}^*$ (cm)	$(\bar{x},\bar{y})$ (cm)	$\sigma_x$ (cm)	$\sigma_y$ (cm)	$\sigma_x^2$ (cm)	$\sigma_y^2$ (cm)
Left	(11.5, 91.8)	(13.3, 92.8)	1.66	0.71	2.76	0.50
Center	(25.6, 84.5)	(26.6, 80.9)	0.48	0.15	0.23	0.02
Right	(35.0, 86.4)	(35.3, 86.1)	0.75	0.25	0.57	0.06

Table 2: Mean, standard deviation and variance of the further tests.

Box	$(x,y)_{real}^*$ (cm)	$(\bar{x},\bar{y})$ (cm)	$\sigma_x$ (cm)	$\sigma_y$ (cm)	$\sigma_x^2$ (cm)	$\sigma_y^2$ (cm)
1	(35.5, 54.0)	(32.9, 53.9)	0.27	0.26	0.07	0.06
2	(19.0, 111.2)	(20.6, 110.8)	2.47	0.65	6.10	0.43

\*Coordinates based on the object's center.

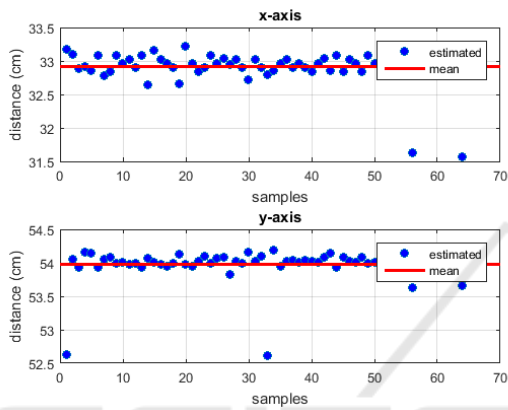


Figure 15: Dispersion of the x-axis and the y-axis samples about the mean value of the first box.

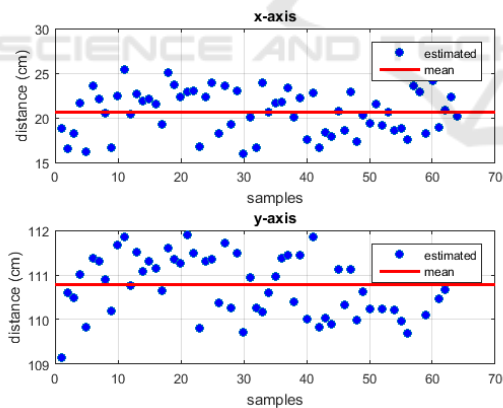


Figure 16: Dispersion of the x-axis and the y-axis samples about the mean value of the second box.

system can recognize them as a single object. In this way, in our test the objects were positioned far from each other. One of the objects used was the same one described in Subsection 6.1 and the other was a medium cardboard box. The procedures in Subsection 6.1 were repeated. The positioning of both objects was random, the smaller box (Box 1) was closer to the sensors and the larger box (Box 2) further away. The standard deviation ( $\sigma$ ), mean ( $(\bar{x},\bar{y})$ ) and variance

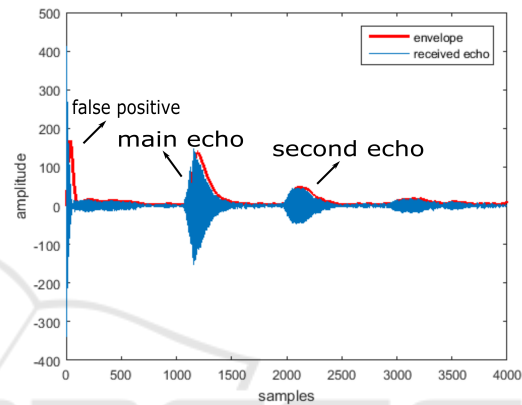


Figure 17: Example of an echo signal received.

( $\sigma^2$ ) of each situation are presented in Table 2. Figures 15, 16 show the variation of the samples in relation to the mean of each measurement.

Figure 17 shows a frequent error in the receivers. The target was more than 1 cm apart, however the system indicated that the object was at a smaller distance. The problem seems to occur because the echo signal interferes with a signal that travels directly from the transmitter to the receiver, without reflecting on the object. Then, in an attempt to reduce the direct signal, tubes were added at the receivers and at the transmitter.

## 7 CONCLUSION AND FUTURE WORK

The use of sonar devices is a common approach in mobile robotics. The difficulty of correctly interpreting the acquired data, is actually a problem. This paper focused on the improvement and development of a low cost obstacle location system based on ultrasonic sensors and signal processing techniques.

The selection of an appropriate method to determine the accuracy of the system was one of the diffi-

culties encountered in the execution of this work. Due to the wide beam of the sensor, the point at which the ultrasonic wave reflects on the object is unknown, made the comparison of coordinates calculated by the system with the real coordinates a complex definition.

In Tables 1 and 2 the  $x$  and  $y$  coordinates of the center of the object were used as real only to have a comparison reference with the mean of the samples. After the tests were carried out, it was verified that all the coordinates estimated by the system were contained in the established perimeter. From results, it is clear that the system had good performance, the mean error for the first and second scenario was 1.68% and 1.19% respectively. The worst case occurred in the detection of the second object, because the distance was greater and consequently the dispersion of the points as well.

As future work, it is intended to optimize the processing time with another microcontroller or even a Digital Signal Processor (DSP) for real-time applications, and embed all to some mobile navigation device for testing and system validation. In general, the binaural sensor system through the envelope extraction can be an attractive alternative to the traditional models of ultrasonic detection, presenting good accuracy and repeatability of the measurements.

## ACKNOWLEDGEMENTS

This work is financed by the ERDF — European Regional Development Fund through the Operational Programme for Competitiveness and Internationalisation — COMPETE 2020 Programme within project POCI-01-0145-FEDER-006961, and by National Funds through the FCT — Fundação para a Ciência e a Tecnologia (Portuguese Foundation for Science and Technology) as part of project UID/EEA/50014/2013.

## REFERENCES

- Bényi, Á. (2003). 87.47 a heron-type formula for the triangle. *The Mathematical Gazette*, 87(509):324–326.
- Cheeke, J. D. N. (2016). *Fundamentals and applications of ultrasonic waves*. CRC press.
- Gearhart, C., Herold, A., Self, B., Birdsong, C., and Slivovsky, L. (2009). Use of ultrasonic sensors in the development of an electronic travel aid. In *2009 IEEE Sensors Applications Symposium*, pages 275–280. IEEE.
- Huang, K.-N. and Huang, Y.-P. (2009). Multiple-frequency ultrasonic distance measurement using direct digital frequency synthesizers. *Sensors and Actuators A: Physical*, 149(1):42–50.
- Jackson, J. C., Summan, R., Dobie, G. I., Whiteley, S. M., Pierce, S. G., and Hayward, G. (2013). Time-of-flight measurement techniques for airborne ultrasonic ranging. *IEEE transactions on ultrasonics, ferroelectrics, and frequency control*, 60(2):343–355.
- Kim, H.-S. and Choi, J.-S. (2008). Advanced indoor localization using ultrasonic sensor and digital compass. In *2008 International Conference on Control, Automation and Systems*, pages 223–226. IEEE.
- Kreczmer, B. (2010). Objects localization and differentiation using ultrasonic sensors. In *Robot Localization and Map Building*. IntechOpen.
- Kuc, R. and Siegel, M. W. (1987). Physically based simulation model for acoustic sensor robot navigation. *IEEE Transactions on Pattern Analysis and Machine Intelligence*, (6):766–778.
- Lim, J., Lee, S. J., Tewolde, G., and Kwon, J. (2014). Ultrasonic-sensor deployment strategies and use of smartphone sensors for mobile robot navigation in indoor environment. In *IEEE International Conference on Electro/Information Technology*, pages 593–598. IEEE.
- Marioli, D., Narduzzi, C., Offelli, C., Petri, D., Sardini, E., and Taroni, A. (1992). Digital time-of-flight measurement for ultrasonic sensors. *IEEE Transactions on Instrumentation and Measurement*, 41(1):93–97.
- Patkar, A. R. and Tasgaonkar, P. P. (2016). Object recognition using horizontal array of ultrasonic sensors. In *2016 International Conference on Communication and Signal Processing (ICCSP)*, pages 0983–0986. IEEE.
- Peremans, H., Audenaert, K., and Van Campenhout, J. M. (1993). A high-resolution sensor based on tri-aural perception. *IEEE transactions on Robotics and Automation*, 9(1):36–48.
- Popelka, M., Struška, J., and Struška, M. (2016). Using ultrasonic sensors to create 3d navigation model of area with ultrasonic sensors. *International Journal of Circuits, Systems and Signal Processing*.
- Queirós, R., Martins, R., Girao, P. S., and Serra, A. C. (2006). A new method for high resolution ultrasonic ranging in air. *Proc. international measurement confederation, Rio de Janeiro*.
- Schillebeeckx, F., De Mey, F., Vanderelst, D., and Peremans, H. (2011). Biomimetic sonar: Binaural 3d localization using artificial bat pinnae. *The International Journal of Robotics Research*, 30(8):975–987.
- Wu, C.-J. and Tsai, C.-C. (2001). Localization of an autonomous mobile robot based on ultrasonic sensory information. *Journal of Intelligent and Robotic Systems*, 30(3):267–277.
- Xu, B., Yu, L., and Giurgiutiu, V. (2009). Advanced methods for time-of-flight estimation with application to lamb wave structural health monitoring. In *Proc. International Workshop on SHM*, pages 1202–1209.